Because the oscillator strength associated with the resonant transition is nearly unity for the alkalis, Eq. (A9) is virtually equivalent to

$$\langle 0|z|k\rangle^2=(\hbar^2/2m\bar{E}),\quad k=1_z \qquad (A10)$$
$$=0,\quad k\neq 1_z.$$

Consequently, the relation

$$z|0\rangle\approx((\hbar^2/2m\bar{E}))^{1/2}|1_z\rangle \qquad (A11)$$

holds in regions where $|0\rangle$ is appreciable. Accordingly, for $z=R$, the ratio of $|1_z\rangle$ to $|0\rangle$ is

$$c(R)=R\left(\frac{2m\bar{E}}{\hbar^2}\right)^{1/2}=\left(\frac{R}{a_0}\right)\left(\frac{\bar{E}}{E_H}\right)^{1/2}. \qquad (A12)$$

Combining Eqs. (A12) and (A5), we finally obtain for Λ

$$\Lambda(R)=-\frac{R}{a_0}\frac{\Delta E_{s.r.}(R)}{(\bar{E}E_H)^{1/2}}. \qquad (A13)$$

PHYSICAL REVIEW VOLUME 136, NUMBER 6A 14 DECEMBER 1964

One-Dimensional Electron-Phonon Model*

STANLEY ENGELSBERG AND B. B. VARGA†
Palmer Physical Laboratory, Princeton University, Princeton, New Jersey
(Received 2 July 1964)

The properties of a one-dimensional system of degenerate electrons coupled to long-wavelength phonons are investigated. The equivalent model Hamiltonian of Tomonaga, which describes the electrons by density waves, is diagonalized to normal modes. These are calculated for the Einstein model and constant coupling, and used to get the ground-state energy. A physical interpretation of the model is given. The breakdown of the system for strong coupling is discussed. The many-body perturbation theory is used to assess the validity of the Tomonaga model. The electron-phonon ground-state energy diagrams may be grouped in two sets as Tomonaga and non-Tomonaga. The latter cancel among themselves exactly to a high order. The extent of the cancellation in three dimensions is treated in fourth order and found to be significant, but not exact.

1. INTRODUCTION

THE properties of an electron-phonon system are investigated for the case when the electrons are degenerate and the shortest wavelength coupled phonon has wave vector k_c much smaller than the Fermi momentum k_f. For these phonons the wavelength is large compared to the average electron spacing, and the electron density fluctuations which couple to the phonons are well-defined collective "sound" waves. Most of the work is on a one-dimensional model; Sec. 10 discusses the possibility of extending the results to three dimensions.

The method of Tomonaga[1] is used in Sec. 2 to derive an equivalent Hamiltonian for the system where the electron kinetic energy for momentum p is $v_f|p|$. The electron kinetic energy operator is expressed in terms of boson operators which create and annihilate electron density waves. The validity of the description of the electron-phonon system by the Tomonaga Hamiltonian is discussed using Tomonaga's results, and an extension is given which is proved by perturbation methods in Sec. 7. The physical interpretation of the boson kinetic operator in Sec. 3 splits the operator into two parts. The first gives the Fermi-Thomas energy of degenerate electrons with long-wavelength density oscillations; the second is the energy of the collective motion in these oscillations. We may consider the description to be a dynamical Fermi-Thomas method which accounts for the correlations in the long-wavelength motions of the electron gas.

The Tomonaga Hamiltonian is diagonalized by a canonical transformation in Sec. 4 into a set of independent harmonic oscillators, three for each wave vector when the electron spin is included as a variable. One of the independent modes is a spin density wave whose frequency is unaffected by the phonons, because it leads to no change in the electron density in space. The dispersion curves of the oscillators are calculated in a specific model: Einstein-model phonons of frequency ω, and the electron-phonon vertex matrix elements g_k taken as constant$=g$ for $|k|<k_c$ and zero for $|k|>k_c$. When $\Omega_k=v_f|k|$ is not close to ω, the two other displaced normal modes contain a phonon and a density wave with no spin wave, one of the modes being mainly a phonon and the other mainly a density wave. For $v_f|k|$ close to ω, neither mode is mainly phonon or density fluctuation. The mode which is a phonon (density wave) for $\Omega_k\ll\omega$ becomes a density wave (phonon) for $\Omega_k\gg\omega$.

The ground-state energy E_T of the system is plotted against the coupling strength g and the cutoff momentum k_c. It is shown that in the general case, E_T is analytic in the coupling constant, so that perturbation

* Work supported in part by a DuPont Research grant.
† Leeds and Northrup Foundation Predoctoral Fellow.
[1] S. Tomonaga, Progr. Theoret. Phys. (Kyoto) 5, 544 (1950).

theory is valid for coupling strength smaller than the critical coupling, beyond which the Tomonaga Hamiltonian has no lowest eigenvalue.

The behavior of the system beyond critical coupling is considered in Sec. 5. For coupling slightly less than critical, the number of phonons and density waves present in the system increases rapidly, and the Tomonaga Hamiltonian no longer gives a good description of the electron-phonon system. With the use of a variational wave function it is shown that above critical coupling the binding energy goes as the square of the number of electrons. The wave function also suggests the collapse of the electrons into a region of length comparable to $2\pi/k_c$.

The perturbation-theory rules for the ground-state energy diagrams of the system are given in Sec. 6, in both the electron and the density wave pictures. An argument is given in Sec. 7 that the two perturbation series must agree to order $2k_f/k_c$ in the coupling strength. The Tomonaga or "bubble" diagrams have the form of electron-hole pair bubbles linked to phonons at the ends. The electron-phonon perturbation series contains the Tomonaga diagrams as a subset. If the two series agree, the extra diagrams must cancel in each order. They are first present in fourth order, where the cancellation is demonstrated explicitly. In Sec. 8 the perturbation rules for the electron distribution in momentum space are given. It is shown that the non-Tomonaga diagrams do not cancel for this property, because the Tomonaga diagrams only affect the distribution in the momentum interval k_f-k_c to k_f+k_c, while it is evident that higher orders of perturbation lead to particles well above k_f and holes well below.

The Green's function method is used to calculate the Tomonaga energy in Sec. 9. It is pointed out that the phonon self-energy calculated from the lowest order diagram is actually correct to order $2k_f/k_c$. This is not true of the electron self-energy.

The last section discusses the possibility of extending the results to three dimensions by analyzing the fourth-order ground-state energy diagrams. The non-Tomonaga diagrams no longer cancel exactly. It is shown from phase space considerations that the "bubble" diagrams dominate in the high-density region,[2] where $k_f \gg k_c$, so that in fourth order the phase space alone reduces a non-Tomonaga diagram as compared to Tomonaga by a factor $(k_c/k_f)^2$, however when the non-Tomonaga diagrams are added, the total is down by a factor $(k_c/k_f)^3$.

2. REVIEW OF THE TOMONAGA MODEL

Tomonaga showed that a one-dimensional assembly of degenerate free electrons can be described by a quantized field of density waves obeying Bose statistics.[1] This section reviews the results of Tomonaga and discusses the validity of his model. The density wave description is a convenient starting point for treating the properties of phonons coupled to density waves of the same wave vector k.[3] We assume that only phonons of long wavelength are coupled, so that $|k|<k_c$, where k_c is the cutoff wave vector. The length $\lambda_c=2\pi/k_c$ is taken large compared to the length which contains one electron on the average, so the electron density varies smoothly within the density waves. This means $k_c \ll k_f$, where k_f is the Fermi momentum of the free electrons.

The system is on a line of length L with periodic boundary conditions. The second quantized electron field operator for spin σ at the point x may be written in terms of plane-wave amplitudes

$$\psi_\sigma(x)=\sum_k L^{-1/2}e^{ikx}c_{k,\sigma}, \quad k=2\pi n/L, \quad n=0,\pm1,\cdots. \tag{2.1}$$

The density operator $\rho_\sigma(x)=\psi_\sigma^*(x)\psi_\sigma(x)$ has the plane wave amplitude

$$\rho_{k,\sigma}=\int_0^L L^{-1/2}e^{-ikx}\rho_\sigma(x)dx = L^{-1/2}\sum_q c_{q-k/2,\sigma}^* c_{q+k/2,\sigma}. \tag{2.2}$$

It is convenient to take the free-electron energy as $\epsilon_p=v_f|p|$, where v_f is the Fermi velocity. Let S be the space of many-electron wave functions such that the single electron levels deep in the Fermi sea between momenta $-\frac{3}{2}k_c$ and $+\frac{3}{2}k_c$ are fully occupied. The operators ρ_k, $|k|<k_c$ (spin index omitted) have a simple time behavior when acting within the space S.

$$\rho_k(t)=\rho_k^+\exp(-iv_fkt)+\rho_k^-\exp(iv_fkt),$$
$$\rho_k^\pm=L^{-1/2}\sum_{\pm q>0} c_{q-k/2}^* c_{q+k/2}. \tag{2.3}$$

For $k>0$, ρ_k^- behaves exactly as a creation operator and ρ_k^+ as an annihilation operator, while for $k<0$ they are reversed. The "quanta" of these operators are density waves made up of particle-hole pairs excited from the Fermi sea, which all propagate in phase with velocity $\pm v_f$ because of the choice of ϵ_k. The commutation rules of these operators within S are best expressed in terms of the properly normalized boson creation and annihilation operators.

$$a_{k,\sigma}=(2\pi/|k|)^{1/2}\rho_{k,\sigma}^\pm, \quad k\gtrless 0,$$
$$a_{k,\sigma}^*=(2\pi/|k|)^{1/2}\rho_{-k,\sigma}^\pm \quad k\gtrless 0, \tag{2.4}$$

$$[a_{k,\sigma},a_{k',\sigma'}]=0, \quad [a_{k,\sigma},a_{k',\sigma'}^*]=\delta_{k,k'}\delta_{\sigma,\sigma'}. \tag{2.5}$$

[2] N. Hugenholtz, Physica 23, 533 (1957).

[3] Several papers have been written on the application of the Tomonaga model to an electron-phonon system. G. Wentzel, Phys. Rev. 83, 168 (1951); J. Bardeen, Rev. Mod. Phys. 23, 261 (1951); K. Huang, Proc. Phys. Soc. (London) A64, 867 (1951); Y. Kitano and H. Nakano, Progr. Theoret. Phys. (Kyoto) 9, 370 (1953).

The kinetic-energy operator of the electrons,

$$K=\sum_{p,\sigma}\epsilon_p c_{p,\sigma}{}^* c_{p,\sigma}. \tag{2.6}$$

may be written in terms of the boson operators:

$$K=T'+H_0', \tag{2.7}$$

where

$$H_0'=2\sum_{1k1<k_f}\epsilon(k) \tag{2.8}$$

is the energy of the filled Fermi sea, and

$$T'=\sum_{1k1<k_f/2,\sigma}\Omega_k a_{k,\sigma}{}^* a_{k,\sigma},\quad \Omega_k=v_f|k|. \tag{2.9}$$

Tomonaga proved that (2.7) is an equality within a subspace S' of states characterized by having no holes below absolute momentum $\frac{3}{4}k_f$ and no electrons above $(5/4)k_f$. All the operators in (2.9) have boson commutation rules within S', which is a subspace of S. The density wave operators in Eq. (2.9) with label $|k|>k_c$ are not coupled to phonons and do not play a role in the dynamics of the system. We may define a kinetic operator in which these are omitted.

$$T=\sum_{1k1<k_c}\Omega_k a_{k,\sigma}{}^* a_{k,\sigma}. \tag{2.10}$$

We shall consider the validity of the model within the context of perturbation theory. Let ψ be an eigenstate of the coupled system which is obtained by perturbation theory from ψ_0, an eigenstate of free density waves and phonons. In the perturbation expansion of ψ the low-order terms will have no holes present in the small-momentum region, so they are in the space S. It is shown in Sec. 7 that for the parts of ψ in S, the operator T acts exactly as $K-H_0'$. Choose ψ to be the ground state and ψ_0 the Fermi sea. The part of ψ coming from perturbation order up to but not beyond $\frac{1}{4}k_f/k_c$ is in S', while the corresponding order for S is k_f/k_c. From the viewpoint of perturbation theory the model is valid to a higher order than indicated by the criterion of Tomonaga. The critical factor is that the main part of ψ be in S, so that there are few holes at small momenta. If this is not the case, the model ground state is not close to the ground state of the electron-phonon system. In the case of weak coupling the excited electrons and holes will be mostly in a small region of momentum space about $\pm k_f$, where the second derivative of the usual electron kinetic energy $p^2/2m$ may be neglected. The excitation energy of an electron or hole measured from the Fermi energy is then $v_f|p-p_f|$, and the free-electron energy spectrum $\epsilon_p=v_f|p|$ leads to the same ground-state wave function.

3. PHYSICAL INTERPRETATION OF THE TOMONAGA HAMILTONIAN

The excitation kinetic-energy operator T is a sum of independent harmonic oscillators, each of which may be separated into a "kinetic" and a "potential" energy term by introducing coordinate and momentum operators

$$\begin{aligned} Q_{k,\sigma}&=(2\Omega_k)^{-1/2}(a_{k,\sigma}+a_{-k,\sigma}{}^*),\\ P_{k,\sigma}&=-i(\Omega_k/2)^{1/2}(a_{k,\sigma}-a_{-k,\sigma}{}^*), \end{aligned} \tag{3.1}$$

$$T=\tfrac{1}{2}\sum_{1k1<k_c,\sigma}(P_{k,\sigma}{}^* P_{k,\sigma}+\Omega_k{}^2 Q_{k,\sigma}{}^* Q_{k,\sigma}-\Omega_k). \tag{3.2}$$

The "potential" energy represents the energy needed to compress a degenerate Fermi gas when a density wave propagates. The "kinetic" energy comes from the collective motion of the large number of electrons within each wavelength of the density wave.

From the definitions (2.3) and (2.4) the potential energy is

$$V=\tfrac{1}{2}\sum_{k,\sigma}\Omega_k{}^2 Q_{k,\sigma}{}^* Q_{k,\sigma}=\frac{1}{L}\sum_{1k1<k_c,\sigma}\tfrac{1}{2}\pi v_f\rho_{k,\sigma}\rho_{-k,\sigma}. \tag{3.3}$$

In the electron-phonon system only the long wavelengths play a role, and we may imagine the restriction on k in (3.3) to be removed in order to write V in coordinate space.

$$V=\tfrac{1}{2}\pi v_f\sum_\sigma\int_0^L(\rho_\sigma{}^2(x)-\bar{\rho}_\sigma{}^2)dx. \tag{3.4}$$

The term containing $\bar{\rho}_\sigma$, the average density of electrons of either spin, comes from the absence of $k=0$ in (3.3).

It has been pointed out by Huang[3] that the Thomas-Fermi method[4] is relevant for a physical interpretation. This statistical method ascribes a possible electron state to each "cell" of phase space of size $\Delta p\Delta x=h$. The statistical energy belonging to a length Δx of the system is obtained by adding the kinetic energies of electrons in the occupied cells. The cells are occupied up to the local Fermi level, which depends on the local density. The statistical energy found this way is the first term of (3.4), which shows that it is the extra energy due to density fluctuations.

When a long-wavelength λ density wave propagates through the system, a region $\Delta x<\lambda$ still contains many electrons so that the electron gas has a well-defined average velocity. In the rest frame of the particles in this region, the cells are occupied to the local Fermi level, but in the laboratory frame the occupied cells are seen to be displaced in momentum and centered about the average momentum. Let $\rho_\sigma(x,+)$ and $\rho_\sigma(x,-)$ be operators which measure the density of those electrons at a point x which are moving to the right and left, respectively. The statistical energy of the region Δx,

[4] F. Seitz, *Modern Theory of Solids* (McGraw-Hill Book Company, Inc., New York, 1940), pp. 384.

taking the average motion into account, is

$$\sum_\sigma \pi v_f[\rho_\sigma^2(x,+)+\rho_\sigma^2(x,-)].$$

On subtracting the potential energy V we obtain the kinetic energy W of collective motion.

$$W=\tfrac{1}{2}\pi v_f\sum_\sigma\int[\rho_\sigma(x,+)-\rho_\sigma(x,-)]^2dx. \quad (3.5)$$

We show this is the first term of (3.2).

The expectation value of $\rho(x,+)$ in a one-electron state $\varphi(x)$ is $|\varphi^+(x)|^2$, where

$$\varphi(x)=\int_{-\infty}^{\infty}\varphi(k)e^{ikx}dk,$$

and

$$\varphi^+(x)=\int_0^\infty\varphi(k)e^{ikx}dk$$

is the part of φ which represents a particle moving to the right. In the second-quantized form,

$$\begin{aligned}\rho(x,+)&=\frac{1}{L}\sum_{m>0,n>0}c_m^*c_ne^{i(n-m)x}\\&=\frac{1}{L}\sum_{l>0,-l<k/2<l}c_{l-k/2}^*c_{l+k/2}e^{ikx}.\end{aligned} \quad (3.6)$$

For $l<\frac{1}{2}k_c$, the creation operator acting on a state in S gives zero. Since the only density wavelengths of importance in the problem are longer than λ_c, the sum for $k>k_c$ in (3.6) is unimportant, and the restriction on k can be dropped.

$$\rho(x,+)\doteqdot\frac{1}{L}\sum_{l>0,|k|<k_c}c_{l-k/2}^*c_{l+k/2}e^{ikx} \quad (3.7)$$

and similarly

$$\rho(x,-)\doteqdot\frac{1}{L}\sum_{l<0,|k|<k_c}c_{l-k/2}^*c_{l+k/2}e^{ikx}. \quad (3.8)$$

The "kinetic" energy from (3.2) is

$$\begin{aligned}W'&=\tfrac{1}{2}\sum_{|k|<k_c,\sigma}P_{k,\sigma}^*P_{k,\sigma}\\&=\tfrac{1}{2}\pi v_f\sum_{|k|<k_c,\sigma}(\rho_{k,\sigma}^+-\rho_{k,\sigma}^-)^*(\rho_{k,\sigma}^+-\rho_{k,\sigma}^-).\end{aligned} \quad (3.9)$$

Define

$$\begin{aligned}\Pi_\sigma(x)&=L^{-1/2}\sum_{|k|<k_c}(\rho_{k,\sigma}^+-\rho_{k,\sigma}^-)e^{ikx}\\&=\frac{1}{L}\sum_{|k|<k_c}e^{ikx}\Big(\sum_{l>0}c_{l-k/2,\sigma}^*c_{l+k/2,\sigma}\\&\qquad-\sum_{l<0}c_{l-k/2,\sigma}^*c_{l+k/2,\sigma}\Big)\\&=\rho_\sigma(x,+)-\rho_\sigma(x,-).\end{aligned} \quad (3.10)$$

Again the restriction $|k|<k_c$ may be removed in (3.9), and

$$W'=\tfrac{1}{2}\pi v_f\sum_\sigma\int_0^L\Pi_\sigma^2(x)dx=W.$$

The operator T gives a better description of the dynamics of the degenerate electron gas than the simple statistical method which keeps only the term V, since the correlations between electrons moving in density waves are taken into account in W. The zero-point oscillator energies in (3.2) were not obtained by these quasiclassical arguments.

The interpretation suggests that the degenerate electron gas in three dimensions cannot be described by a quadratic form constructed from density wave operators. For example, with the electron kinetic energy $p^2/2m$ the expression for V is

$$\int(20\pi^2m)^{-1}\sum_\sigma(6\pi^2\rho_\sigma(\mathbf{x}))^{5/3}d^3x.$$

4. GROUND-STATE ENERGY

In this section we calculate the ground-state energy for an electron-phonon system. The interaction to first order in the lattice displacement couples the longitudinal lattice normal-mode coordinate $q_k=q_{-k}^*$ of wave vector k to the density wave $\rho_{-k,\sigma}$ with matrix element $g_k=g_{-k}=g_k^*$.

$$\begin{aligned}H_I&=\sum_{k,\sigma}g_k\rho_{-k,\sigma}q_k\\&=\sum_{k,\sigma}g_k(|k|/2\pi)^{1/2}(a_{k,\sigma}^*q_k+a_{k,\sigma}q_k^*),\end{aligned} \quad (4.1)$$

where ω_k is the frequency of the bare phonon. The noninteracting phonon part of the Hamiltonian is

$$H_S=\tfrac{1}{2}\sum_k(p_k^*p_k+\omega_k^2q_k^*q_k), \quad (4.2)$$

where p_k^* is canonically conjugate to the phonon coordinate q_k.

$$[q_k,p_{k'}^*]=i\delta_{k,k'}.$$

The total Hamiltonian in the Tomonaga approximation (2.8), (2.10) is

$$H_T=H_0'+T+H_S+H_I=\sum_k H_k, \quad (4.3)$$

where the individual H_k commute.

The Hamiltonian (4.3) can be diagonalized exactly. We make the canonical transformation (3.1) introducing the operators $Q_{k,\sigma}$ and $P_{k,\sigma}$ which obey the canonical commutations relations

$$[Q_{k,\sigma},P_{k',\sigma'}^*]=i\delta_{k,k'}\delta_{\sigma,\sigma'}.$$

Under this transformation the kinetic operator becomes

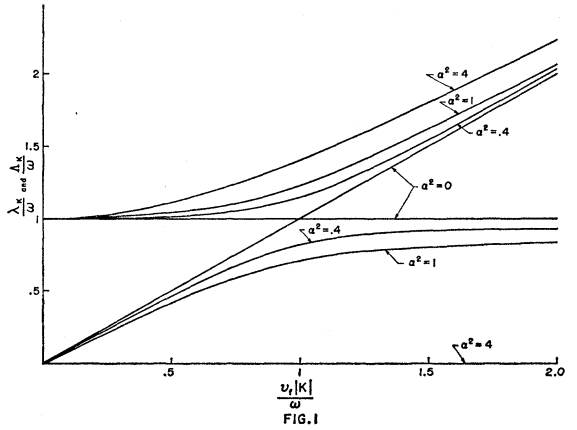

FIG. 1. The excitation spectra Λ_k/ω, λ_k/ω, Ω_k/ω of the interacting system as a function of $v_f|k|/\omega$ for various values of the coupling constant α^2. The excitation spectra of the noninteracting system Ω_k/ω and ω_k/ω are also included to illustrate the splitting of the modes when the interaction is turned on.

(3.2) and the interaction operator becomes

$$H_I=\sum_{k,\sigma}(|k|\Omega_k/4\pi)^{1/2}g_k(q_k^*Q_{k,\sigma}+q_kQ_{k,\sigma}^*). \quad (4.4)$$

An orthogonal transformation on the vectors

$$\Pi_k=\begin{bmatrix}P_{k\uparrow}\\P_{k\downarrow}\\p_k\end{bmatrix}$$
$$\Phi_k=\begin{bmatrix}Q_{k\uparrow}\\Q_{k\downarrow}\\q_k\end{bmatrix} \quad (4.5)$$

diagonalizes the Hamiltonian H_T. In terms of the new vectors, whose components are canonical,

$$\Pi_k'=R_k\Pi_k,$$
$$\Phi_k'=R_k\Phi_k, \quad (4.6)$$

the Hamiltonian is

$$H_T=H_0'-\textstyle\sum_k\Omega_k+\frac{1}{2}\sum_k(\Pi_k'^\dagger\Pi_k'+\Phi_k'^\dagger M_k^2\Phi_k'), \quad (4.7)$$

where the matrix M_k^2 is diagonal:

$$M_k^2=\begin{bmatrix}\Omega_k^2&0&0\\0&\Lambda_k^2&0\\0&0&\lambda_k^2\end{bmatrix} \quad (4.8)$$

with

$$\Lambda_k^2=\tfrac{1}{2}\{\omega_k^2+\Omega_k^2+[(\omega_k^2-\Omega_k^2)^2+\alpha_k^2\omega_k^2\Omega_k^2]^{1/2}\} \quad (4.9)$$

and

$$\lambda_k^2=\tfrac{1}{2}\{\omega_k^2+\Omega_k^2-[(\omega_k^2-\Omega_k^2)^2+\alpha_k^2\omega_k^2\Omega_k^2]^{1/2}\}. \quad (4.10)$$

The excitation energies of the system, Λ_k and λ_k, are plotted in Fig. 1, for the model in which we have optical phonons, $\omega_k=\omega$ and constant coupling $\alpha_k^2=\alpha^2$.

The quantity α_k^2 appearing in the eigenvalues is a dimensionless coupling term

$$\alpha_k^2=16g_k^2N(0)/\omega_k^2, \quad (4.11)$$

where $N(0)=1/2\pi v_f$ is the density of electron states of one spin at the Fermi level.

The transformation matrix R has for its three rows the components of the three orthonormal vectors

$$e_1=(2)^{-1/2}\{1,-1,0\},$$
$$e_2=[2(\omega^2-\Lambda^2)^2+\alpha^2\Omega^2\omega^2/2]^{-1/2}\times\{\omega^2-\Lambda^2,\omega^2-\Lambda^2,-\alpha\Omega\omega/\sqrt{2}\}, \quad (4.12)$$
$$e_3=[2(\omega^2-\lambda^2)^2+\alpha^2\Omega^2\omega^2/2]^{-1/2}\times\{\omega^2-\lambda^2,\omega^2-\lambda^2,-\alpha\Omega\omega/\sqrt{2}\},$$

where we have suppressed the momentum index.

It is interesting to note that one of the normal modes of the Hamiltonian oscillates with the unperturbed frequency of the density fluctuations Ω_k. The transformation vector e_1 shows that this mode is a spin wave, that is a linear combination of spin-up and spin-down density fluctuations having equal amplitudes and opposite phases. With the Hamiltonian in the form (4.7) we may immediately write an expression for the ground-state energy

$$F_0'=H_0'+\tfrac{1}{2}\textstyle\sum_k(\Lambda_k+\lambda_k-\Omega_k). \quad (4.13)$$

As pointed out by Wentzel and Bardeen,[3] the root λ_k becomes imaginary for $\alpha_k^2>4$.

The lowering of the ground-state energy by the interaction

$$E_T=F_0'-H_0'-\tfrac{1}{2}\textstyle\sum_k\omega_k=\tfrac{1}{2}\sum_k(\Lambda_k+\lambda_k-\Omega_k-\omega_k) \quad (4.14)$$

is plotted in Figs. 2, 3, and 4 for the constant-coupling, optical-phonon model. As mentioned earlier the momentum transfer to the phonons in the interaction is taken to have a cutoff k_c. This limits, the maximum Ω_k to $v_fk_c=x\omega$. The quantity x introduced above should certainly be chosen greater than 1, since it is just at this value that the unperturbed modes Ω_k and ω crossed. In Fig. 2 we plot the energy lowering E_T as a function of x for $\alpha_k^2=1$, an intermediate-coupling case.

In Figs. 3 and 4 E_T is plotted as a function of coupling constant for $x=2$ and 4. For values of $x>4$, the extra contribution to the energy lowering is coming almost entirely from the depression of the lower mode energy from ω to $\lambda\rightarrow\omega(1-\alpha^2/4)^{1/2}$ for $\Omega_k\gtrsim4\omega$. The physically important effect of the electron-phonon interaction is the splitting of the modes, which is largest at $\Omega_k=\omega$.

The electron-phonon interaction also changes the specific heat of the system. As pointed out by Wentzel,[3] the low-temperature specific heat of the free electrons is identical with that of the free density waves, as expected from Sec. 2. Only the low-lying modes, which have longest wavelength, contribute to the low-temperature specific heat, and the result is

$$C_V=(4/3)\pi^2N(0)k_B^2T,$$

where k_B is Boltzmann's constant.

When the interaction is turned on, one of the two

low-lying modes with energy Ω_k is lowered to energy λ_k, which for very long wavelengths is

$$\lambda_k|_{k\to 0} \to \Omega_k(1-\alpha^2/4)^{1/2}.$$

We can state the results for the specific heat of the interacting system in terms of the renormalized density of states of the lowered mode

$$N'(0)=N(0)\,(1-\alpha^2/4)^{-1/2},$$
$$C_V=\tfrac{2}{3}\pi^2 k_B{}^2 T[N(0)+N'(0)].$$

As the coupling constant goes to its critical value, $\alpha^2=4$, the small slope of the mode λ_k leads to a divergent specific heat.

An important point to be noted is that the expression (4.14) for the ground-state energy is analytic in the coupling constant for $\alpha_k{}^2<4$. The only terms that depend upon coupling constant in (4.14) are

$$\Lambda+\lambda=[\tfrac{1}{2}\{\omega^2+\Omega^2+[(\omega^2-\Omega^2)^2+\alpha^2\omega^2\Omega^2]^{1/2}\}]^{1/2}$$
$$+[\tfrac{1}{2}\{\omega^2+\Omega^2-[(\omega^2-\Omega^2)^2+\alpha^2\omega^2\Omega^2]^{1/2}\}]^{1/2}. \quad (4.15)$$

For $\alpha^2<4$

$$a=\omega^2+\Omega^2>[(\omega^2-\Omega^2)^2+\alpha^2\omega^2\Omega^2]^{1/2}=b$$

and we may expand the outer square root in each term

$$\Lambda+\lambda=\left(\frac{a}{2}\right)^{1/2}\left\{\left(1+\frac{b}{a}\right)^{1/2}+\left(1-\frac{b}{a}\right)^{1/2}\right\}$$
$$=\left(\frac{a}{2}\right)^{1/2}\left\{2-\frac{1}{4}\frac{b^2}{a^2}-\frac{5}{64}\frac{b^4}{a^4}-\cdots\right\}. \quad (4.16)$$

Since only even powers of b appear in the expansion (4.16), no terms with square roots arise. Thus there is a power-series expansion of the ground-state energy in terms of the coupling constant. At $\alpha_k{}^2=4$, the derivative of the ground-state energy with respect to coupling constant goes to minus infinity. If we were to continue evaluating the ground-state energy in terms of its power-series expansion for $\alpha_k{}^2$ greater than 4 we would obtain infinite results. The fact that the ground-state energy is analytic in the coupling constant means that within the region of analyticity we could evaluate the ground-state energy of the Tomonaga Hamiltonian by perturbation theory and sum the series to obtain (4.14). We will go into the detailed analysis of the perturbation theory treatment in Sec. 7. However at this stage we may note that contrary to Tomonaga's conjecture,[5] whenever the Tomonaga Hamiltonian is positive definite the results for the ground-state energy do not go beyond the realm of perturbation theory.

This result precludes the comparison of the Tomonaga model with the Bardeen-Cooper-Schrieffer (B.C.S.) model of superconductivity.[6] We cannot compare the two, since the B.C.S. pairing correlations are in addition to any correlations found strictly within perturbation theory. The B.C.S. pairing correlations lead to a lowering of the ground-state energy of the form $\Delta E\propto -N(0)\omega^2\exp[-2\omega^2/N(0)g^2]$. For small enough coupling constant this will be dominated by the lowering due to the collective excitation. A manifestation of the B.C.S. instability within perturbation theory is the existence of an imaginary pole of the T matrix for ladder diagrams.[7] The Tomonaga Hamiltonian does not include these diagrams.

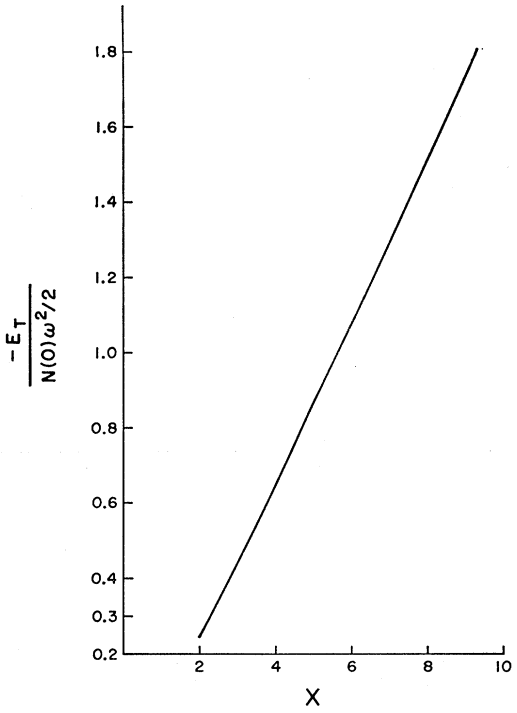

FIG. 2. The energy lowering by the interaction $E_T/\frac{1}{2}N(0)\omega^2$ is plotted as a function of the cutoff $x=v_f k_c/\omega$, with α^2 chosen equal to one.

5. THE BREAKDOWN OF THE SYSTEM

When the coupling constant α^2 approaches the critical value 4 from below, the lower mode λ_k approaches zero for all k. If now α^2 increases beyond 4, $\lambda_k{}^2$ becomes negative, and the spectrum of the Tomonaga Hamiltonian is not bounded from below.[3] In this section we investigate the breakdown and determine whether the electron-phonon system itself is unstable.

The average number of phonons of wave vector k is

$$h_k=\langle b_k{}^* b_k\rangle=(\partial/\partial\omega_k)E_T$$
$$=(\partial/\partial\omega_k)\tfrac{1}{2}(\Lambda_k+\lambda_k-\omega_k-\Omega_k). \quad (5.1)$$

[5] Reference 1, pp. 545–547.

[6] J. Bardeen, L. N. Cooper, and J. R. Schrieffer, Phys. Rev. **108**, 1175 (1957).

[7] C. Bloch, Compt. Rend. Congr. Intern. Phys. Nucl. Paris (1958), p. 243; V. J. Emery, Nucl. Phys. **12**, 69 (1959); L. Van Hove, Physica **25**, 849 (1959); M. L. Mehta, Nucl. Phys. **12**, 333 (1959).

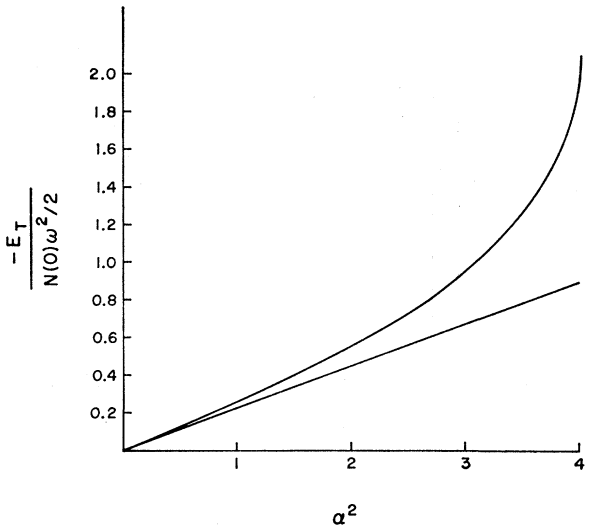

FIG. 3. The energy lowering $E_T/\frac{1}{2}N(0)\omega^2$ as a function of coupling constant α^2 for cutoff $x=2$. The straight line is the result obtained from second-order perturbation theory.

In taking the derivative, the coefficient $\frac{1}{4}\alpha(\Omega\omega/2)^{1/2}$ of the term $(a+a^*)(b+b^*)$ in H_I is to be fixed.

$$h=-\frac{\omega}{4}\left(\frac{1}{\Lambda}+\frac{1}{\lambda}\right)+[\omega(\omega^2-\Omega^2)+\tfrac{1}{4}\alpha^2\omega\Omega^2]\times\left(\frac{1}{4\Lambda(\Lambda^2-\lambda^2)}+\frac{1}{4\lambda(\lambda^2-\Lambda^2)}\right)-\tfrac{1}{2}. \quad (5.2)$$

As $\alpha^2\to 4$ the largest part comes from the terms that go as $1/\lambda$ which came from the derivative of λ

$$h\to\omega\Omega^2/4\lambda\Lambda^2.$$

The large number of phonons in each mode makes the interaction in higher orders of the lattice displacement important in any physical system. Similarly, the average number l_k of bosons of wave vector k and either spin is

$$l_k=\tfrac{1}{2}\textstyle\sum_\sigma\langle a_{k,\sigma}{}^*a_{k,\sigma}\rangle=\tfrac{1}{2}(\partial/\partial\Omega_k)E_T$$
$$=-\frac{\Omega}{8}\left(\frac{1}{\Lambda}+\frac{1}{\lambda}\right)+\tfrac{1}{2}[\Omega(\Omega^2-\omega^2)+\tfrac{1}{4}\alpha^2\omega^2\Omega]\times\left(\frac{1}{4\Lambda(\Lambda^2-\lambda^2)}+\frac{1}{4\lambda(\lambda^2-\Lambda^2)}\right)-\tfrac{1}{4}. \quad (5.3)$$

As $\alpha^2\to 4$, $l\to\Omega\omega^2/8\lambda\Lambda^2$.

As the energy of the lower mode goes to zero, the number of phonons and bosons present in the zero-point motion of the mode blows up as $1/\lambda_k$. The ratio $h_k/2l_k$ is just Ω_k/ω, the inverse ratio of the free mode energies. This follows from (4.12), for the ratio of phonon to boson in the mode e_{3k} is $\alpha\Omega_k\omega/(\omega^2-\lambda_k^2)$ which goes to $2\Omega_k/\omega$ as $\alpha\to 2$. We see that in the collective mode that becomes unstable it is mainly the electrons that break down at low momenta, and mainly the phonons at high momenta, but both participate in every mode to some extent.

Since the system contains many bosons and phonons we may consider the operators $a_k{}^*$, $b_k{}^*$ as c numbers of magnitude $l_k{}^{1/2}$, $h_k{}^{1/2}$, respectively. A classical calculation can be done to determine the critical coupling strength.

$$E_T\doteqdot\sum_{k,\sigma}\Omega_k l_{k,\sigma}+\sum_k\omega h_k-\sum_{k,\sigma}\alpha(\tfrac{1}{2}\omega\Omega)^{1/2}h_k{}^{1/2}l_k{}^{1/2}. \quad (5.4)$$

The relative phase of the c numbers has been chosen as negative so the interaction term has the largest negative value. Since (5.4) is homogeneous, first order, in the variables h_k, l_k, the energy can be scaled arbitrarily by any positive constant. Thus we can only hope to obtain the criterion for breakdown, where (5.4) can first begin to go negative. Fix l_k and vary h_k to minimize (5.4).

$$l_{k,\sigma}/h_k=\tfrac{1}{8}\alpha^2(\omega/\Omega_k),$$
$$E_T=\sum_{k,\sigma}\Omega_k l_{k,\sigma}(1-\alpha^2/4). \quad (5.5)$$

As expected, $\alpha^2=4$ is critical, and $l_k/h_k=\omega/2\Omega_k$.

For a system of finite length L the modes of H_T break down if $\alpha^2>4$. We show now that the electron-phonon system in this length has a lower bound on the energy for arbitrarily strong coupling. This can even be estimated by a simple classical argument. Notice that as the system breaks down, h_k and l_k increase indefinitely. In a system of length L containing

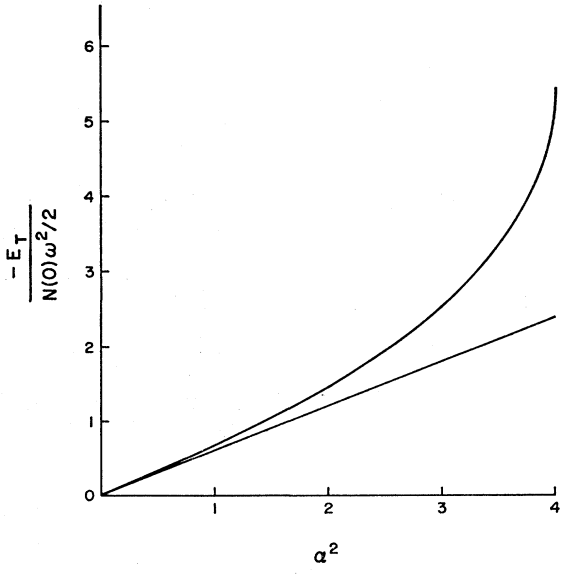

FIG. 4. The energy lowering $E_T/\frac{1}{2}N(0)\omega^2$ as a function of coupling constant α^2 for cutoff $x=4$. As in Fig. 3 we include the result of second-order perturbation theory.

N electrons the maximum eigenvalue of

$$\sum_\sigma (a_{-k,\sigma}+a_{k,\sigma}^*)=\left(\frac{2\pi}{|k|L}\right)^{1/2}\sum_{p,\sigma} c_{p+k/2,\sigma}^* c_{p-k/2,\sigma}$$

$$=\left(\frac{2\pi}{|k|L}\right)^{1/2}\sum_{j=1}^{N} e^{ikr_j}$$

(r_j is the position of the jth electron) is $N(2\pi/|k|L)^{1/2}$, and the maximum l_k is about $\frac{1}{4}\pi N^2/|k|L$. From (5.5) the lowest energy is about

$$(1-\alpha^2/4)\sum_k \Omega_k \pi N^2/2|k|L=(1-\alpha^2/4)$$

$$\times\int \tfrac{1}{4}v_f N^2 dk=N^2(1-\alpha^2/4)x\omega/2. \quad (5.6)$$

The energy depends on N^2 instead of N and is not an extensive quantity.

We may obtain a more precise lower bound by neglecting the kinetic energy which is a positive definite operator, in the electron-phonon Hamiltonian. The eigenstates of the operator $\mathcal{O}=H_I+H_S$ are products of two functions, one of the phonon, the other of the electron coordinates.

$$\psi=\eta(r_j)\chi(q_k). \quad (5.7)$$

The function η is an eigenstate of the commuting set of operators $\rho_k=L^{-1/2}\sum_j e^{-ikr_j}$ with eigenvalues ρ_k'. Then χ satisfies

$$\{\tfrac{1}{2}\sum (p_k^* p_k+\omega^2 q_k^* q_k)+g\sum \rho_{-k}' q_k\}\chi=E_m\chi, \quad (5.8)$$

where E_m is the eigenvalue of $\mathcal{O}$. The lowest E_m is

$$\tfrac{1}{2}\sum_{|k|<k_c}\left(\omega-\frac{g^2}{\omega^2}|\rho_k'|^2\right). \quad (5.9)$$

Choose $|\rho_k'|$ to take the maximum value of $NL^{-1/2}$ for all k, which can be done by placing all electrons at the same point of space. The lower bound is

$$E_l/L=x\omega^2 N(0)[1-\alpha^2 E_f N/\omega]. \quad (5.10)$$

To demonstrate the breakdown of the electron-phonon system we seek an upper bound for E/L which has a term of the form const$\times N$. For large α^2 we expect the constant to be negative. Choose a variational wave function of the form (5.7). The idea is that for strong coupling we can let $\langle\eta|\rho_k|\eta\rangle$ be large for $|k|<k_c$ by placing all the electrons inside a region of width t comparable to $\lambda_c=2\pi/k_c$. The kinetic energy of such a configuration $\eta(r_j)$ of N electrons with spin confined to a box of length $t=\gamma\lambda_c$ is

$$2\sum_{n=0}^{N/2} v_f\frac{n\pi}{t}=\frac{\pi v_f}{t}\left(\frac{N}{2}\right)^2.$$

Take the expectation value of $\mathcal{O}$ in the state $\eta\chi$. The minimum energy is obtained by choosing χ to satisfy (5.8) with ρ_k' replaced by the expectation value $\langle\eta|\rho_k|\eta\rangle=\langle\rho_k\rangle$. The upper bound is

$$E_u/L=x\omega^2 N(0)[1-(\tfrac{1}{4}\alpha^2 g(\gamma)-\tfrac{1}{2}\gamma)E_f N/\omega], \quad (5.11)$$

where

$$g(\gamma)=\sum_{|k|<k_c}|\langle\rho_k\rangle|^2/\sum_{|k|<k_c} N^2/L$$

$$=\sum_{|k|<k_c}|\langle\rho_k\rangle|^2/(N^2 k_c/\pi) \quad (5.12)$$

and $\langle\rho_k\rangle$ is the kth Fourier component of a density function which is N/t inside the length t and zero outside. The discrete sum in (5.12) may be replaced by an integral provided $t\ll L$.

$$g(\gamma)=\frac{4}{t^2 k_c}\int_0^{k_c}\frac{dk}{k^2}\sin^2\frac{kt}{2}$$

$$=-\frac{\sin^2\pi\gamma}{(\pi\gamma)^2}+\frac{1}{\pi\gamma}\,\mathrm{Si}(2\pi\gamma). \quad (5.13)$$

At the critical coupling the coefficient of N in (5.11) is zero and $\alpha_c^2=2/\gamma g(\gamma)$. We shall choose γ to minimize α_c^2. Thus $\gamma g(\gamma)$ is a maximum, which occurs when $\sin\pi\gamma=0$ or $\gamma=\text{integer}=\nu>0$ and

$$\tfrac{1}{2}\gamma g(\gamma)=(1/2\pi)\,\mathrm{Si}(2\pi\nu). \quad (5.14)$$

For example, one maximum occurs at $\nu=8$, where[8] Si is 1.55 and so α_c^2 is 4.05. It is possible to reduce α_c^2 by choosing ν larger and larger, for as $\nu\to\infty$, $\mathrm{Si}\to\pi/2$ and thus $\alpha_c^2\to 4$. This indicates that at $\alpha^2=4$ the system is still distributed over a large region, which however cannot be taken comparable to L, since then $|\langle\rho_k\rangle|^2$ varies so rapidly between the allowed values of k in the sum (5.12) that the integral replacement of the sum is no longer valid.

For $\alpha^2>4$ we minimize $\frac{1}{4}\alpha^2 g(\gamma)-\frac{1}{2}\gamma$, giving

$$\frac{4}{z}\sin^2\frac{z}{2}+\frac{2\pi}{\alpha^2}=\mathrm{Si}(z), \quad z=2\pi\gamma. \quad (5.15)$$

If we let $\alpha^2=2\pi$ the solution for z in (5.15) lies between π and 2π, so t is between $\lambda_c/2$ and λ_c. For larger α^2, t decreases further. We conclude that as α^2 increases beyond 4, the system of electrons rapidly collapses to small dimensions of about λ_c, independent of N. As α^2 continues to increase, t approaches zero as $1/\alpha$, and the interaction term in (5.11) dominates the kinetic term by a factor α, so the upper bound (5.11) approaches the lower bound (5.10).

If the electron energy-momentum relation is $p^2/2m$, the type of trial wave function (5.7) would give a

[8] Natl. Bur. Std., Appl. Math. Ser. 32.

kinetic energy

$$\frac{2}{2m}\sum_{n=0}^{N/2}\left(\frac{n\pi}{l}\right)^2\approx\frac{\pi^2}{3ml^2}\left(\frac{N}{2}\right)^3$$

going as N^3, which gives to E_{II}/L a term going as N^2 with positive coefficient. For large N this term dominates the negative term linear in N. It is evident that the faster increase of ϵ_p with large p acts to prevent the electrons from coming together into a small region of space to take advantage of the large lattice displacement which lowers the energy. As pointed out by Bardeen,[3] this system cannot be approximated by the Tomonaga model when the coupling is strong.

6. PERTURBATION-THEORY RULES

The perturbation-theory rules for the ground-state energy of an electron-phonon system may be derived by the method of Goldstone.[9] A method which combines time-dependent and -independent perturbation theory[10] could also be used. Bloch and De Dominicis have given the rules for the Gibbs function of the system at nonzero temperature.[11]

The Hamiltonian H is the sum of H_0 and H_I of (4.1). In the "electron picture" $H_0=K+H_S$ describes free electrons and phonons, and in the "density wave picture" $H_0=T+H_S$, the electron variables are replaced by density waves. If ψ_0 is the ground state of H_0, the Fermi sea with no phonons, then $e^{-HS}\psi_0$ approaches the ground state ψ of H for large positive S if $(\psi,\psi_0)\neq 0$. The ground-state energy difference of H and H_0 is

$$\Delta E=E-E_0=\lim_{S\to\infty}\langle H_I e^{-HS}\rangle/\langle e^{-HS}\rangle, \qquad (6.1)$$

where $\langle\ \rangle$ denotes expectation values in the state ψ_0.

The expression (6.1) may be written in the interaction representation where, for example, $H_I(S)=e^{H_0S}H_Ie^{-H_0S}$.

$$\Delta E=\lim_{S\to\infty}\left\langle H_I(S)\mathcal{T}\exp-\int_0^S H_I(t)dt\right\rangle\Big/\left\langle\mathcal{T}\exp-\int_0^S H_I(t)dt\right\rangle. \qquad (6.2)$$

$\mathcal{T}$ is the standard ordering operator with respect to the integration parameter, which for convenience shall be called "time." In the electron picture

$$H_I=L^{-1/2}\sum_{p,k,\sigma}g_k(2\omega_k)^{-1/2}c_{p+k,\sigma}{}^*c_{p,\sigma}(b_k+b_{-k}{}^*), \qquad (6.3)$$

where $b_k=(\omega_k/2)^{1/2}q_k+i(2\omega_k)^{-1/2}p_k$ is the phonon annihilation operator and $b_k{}^*$ the creation operator, with boson commutation relations. In the density wave picture

$$H_I=\sum_{k,\sigma}g_k(|k|/4\pi\omega_k)^{1/2}(a_{k,\sigma}{}^*+a_{-k,\sigma})(b_k+b_{-k}{}^*). \qquad (6.4)$$

The equations of motion show that annihilation operators have time dependence like

$$c_p(S)=e^{-\epsilon_pS}c_p,\quad a_k(S)=e^{-\Omega_kS}a_k,$$

and creation operators like $b_k{}^*(S)=e^{\omega_kS}b_k{}^*$.

The perturbation series is obtained by expanding the exponential in (6.2) and using Wick's theorem to evaluate the expectation value of the various terms. The only terms which survive in (6.2) are those in which all contractions are made.

In the electron picture the first term in the numerator of (6.2) is

$$-\left\langle H_I(S)\int_0^S H_I(t)dt\right\rangle$$
$$=-\frac{1}{L}\sum_{p,k,\sigma;p',k',\sigma'}\frac{g_kg_{k'}}{(4\omega_k\omega_{k'})^{1/2}}$$
$$\times\Big\langle c_{p+k,\sigma}{}^*c_{k,\sigma}e^{-(\epsilon_p-\epsilon_{p+k})S}$$
$$\times(b_ke^{-\omega_kS}+b_{-k}{}^*e^{\omega_kS})\int_0^S dtc_{p'+k',\sigma}{}^*c_{p',\sigma'}$$
$$\times e^{-(\epsilon_{p'}-\epsilon_{p'+k'})t}(b_{k'}e^{-\omega_{k'}t}+b_{-k'}{}^*e^{\omega_{k'}t})\Big\rangle. \qquad (6.5)$$

For the phonon contraction the only nonvanishing term is $:b_kb_k{}^*:=1$, and in the electron contraction we must put $(p+k,\sigma)=(p',\sigma')$, $(p,\sigma)=(p'+k',\sigma')$ and obtain 1 if $|p|>k_f$, $|p+k|<k_f$ and 0 otherwise. As $S\to\infty$ only the upper limit of the integral over t in (6.5) is important and the result is

$$-\frac{1}{L}\sum_{|k|<k_c,p,\sigma}\frac{g_k{}^2}{2\omega_k}(\epsilon_p-\epsilon_{p+k}+\omega_k)^{-1} \qquad (6.6)$$

with the restrictions $|p|>k_f$, $|p+k|<k_f$ in the sum. The diagram representing this term is shown in Fig. 5. The straight line going up is a particle outside the Fermi sea, the straight line going down is a hole in the Fermi sea, and the wavy line is a phonon, which may be directed either way. Momentum and spin are conserved at each vertex which contributes a matrix element $g_k/(2\omega_kL)^{1/2}$.

Terms of odd order in H_I from the expansion of (6.2) lead to the contraction of an odd number of phonon operators, which vanishes. In fourth order there are linked as well as unlinked diagrams, with examples shown in Fig. 6. This unlinked diagram gives a contribution to ΔE going as L^2, and therefore must be

[9] J. Goldstone, Proc. Roy. Soc. (London) **A239**, 267 (1957).
[10] C. Bloch, Nucl. Phys. **7**, 451 (1958).
[11] C. Bloch and C. De Dominicis, Nucl. Phys. **7**, 459 (1958).

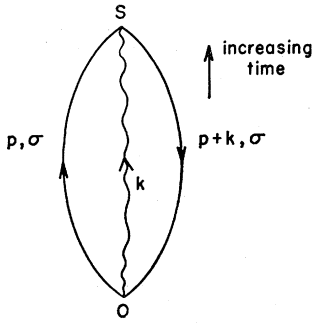

FIG. 5. Second-order ground-state energy diagram in the electron picture.

cancelled by the denominator. An outline of the proof of the linked cluster theorem may be given following Goldstone. All the diagrams in the numerator of (6.2) may be grouped in sets with a common linked subdiagram whose vertex begins at time zero. In one such set fix the time labels on this linked subdiagram and perform the integrals over the other time variables; in the set there are present diagrams in which these time variables take all possible orders with respect to the fixed time labels. If all the members of the set are now added, the result is the special linked subdiagram times a numerical factor equal to the denominator of (6.2). This demonstrates the possibility of expanding ΔE in terms of linked diagrams.

It remains to perform the straightforward time integrations, which lead to energy denominators as in (6.6). We can now state the rules for the evaluation of the contribution of a linked diagram. At each vertex, spin and momentum are conserved, and the matrix element is $g_k/(2\omega_k L)^{1/2}$, where k is the phonon momentum. Write the (positive) excitation energy of each intermediate state in the denominator, multiply by the matrix elements and sum over all the momenta and spins, observing the rule that holes are within the Fermi sea and particles are outside the sea. The sign of the diagram is $-(-1)^P$ where the first-sign comes from expanding the "exp" in the numerator of (6.2) into an odd number of H_I, and P is the parity of the Fermion contraction, which is given by the sum of the numbers of closed electron loops and hole lines.[9]

In the density wave picture the development is quite similar. The first term in the numerator of (6.2) is

$$-\frac{1}{L}\sum_{k,k',\sigma,\sigma'}\frac{g_k g_{k'}}{4\pi}\left(\frac{|kk'|}{\omega_k\omega_{k'}}\right)^{1/2}$$
$$\times\Big\langle(a_{k,\sigma}{}^*e^{\Omega_k S}+a_{-k,\sigma}e^{-\Omega_k S})(b_k e^{-\omega_k S}+b_{-k}{}^*e^{\omega_k S})$$
$$+\int_0^S dt(a_{k',\sigma'}{}^*e^{\Omega_{k'}t}+a_{-k',\sigma'}e^{-\Omega_{k'}t})$$
$$\times(b_{k'}e^{-\omega_{k'}t}+b_{-k'}{}^*e^{\omega_{k'}t})\Big\rangle. \quad (6.7)$$

The only nonzero boson contraction is $:a_{k,\sigma}a_{k,\sigma}{}^*:$. The diagram obtained this way is shown in Fig. 7, where the dashed line indicates a propagating density wave. The result for (6.7) after performing the time integrations is

$$-\sum_{|k|<k_c,\sigma}\frac{g_k{}^2}{2\omega_k}\frac{|k|}{2\pi}(\Omega_k+\omega_k)^{-1}. \quad (6.8)$$

The linked-cluster theorem holds. The contribution of a linked diagram is determined by the same rules as before, but the matrix element at a vertex is $g_k(|k|/4\pi\omega_k)^{1/2}$, and the sum is over all possible momenta less than k_c, since the reference state ψ_0 contains no phonons or density waves. The sign of each diagram is negative.

7. PERTURBATION-THEORY DIAGRAMS

The arguments of Tomonaga show that the model Hamiltonian should describe the properties of the electron-phonon system quite well. The extent to which this is true may be determined by comparing the perturbation series of the two pictures of Sec. 6.

The Brillouin-Wigner perturbation formulas[12] for the ground-state energy and wave function are

$$\psi=\psi_0+BH_I\psi, \quad (7.1)$$

$$\Delta E=\sum_{l=0}^{\infty}\langle H_I(BH_I)^l\rangle, \quad (7.2)$$

$$B=P/(E-H_0), \quad P=1-|\psi_0\rangle\langle\psi_0|, \quad (7.3)$$

where E is the ground-state energy of H and ΔE is the energy shift from the interaction. The electron and the density wave pictures have different forms for the electron kinetic operator, but they lead to the same result when acting on the various terms of (7.1) which are members of S. For example, the second term in the expansion of $|\psi\rangle$ is

$$(P/E-H_0)\sum_k g_k(b_{-k}{}^*a_k{}^*)|\psi_0\rangle. \quad (7.4)$$

A particular term in the sum, $b_{-k}{}^*a_k{}^*|\psi_0\rangle$, is an eigenstate of $K-H_0'$ with eigenvalue $v_f|k|=\Omega_k$. Now

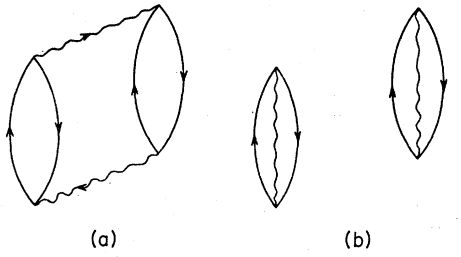

FIG. 6. (a) Linked fourth-order diagram. (b) Unlinked fourth-order diagram.

[12] E. P. Wigner, Math. Naturw. Anz. Ungar. Akad. Wiss. **53**, 475 (1935).

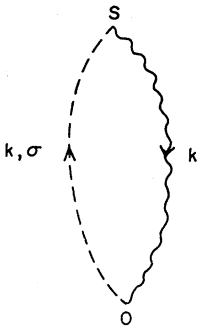

FIG. 7. Second-order ground-state energy diagram in the density wave picture.

consider

$$Tb_{-k}^*a_k^*|\psi_0\rangle=(\sum_{k'}\Omega_{k'}a_{k'}^*a_{k'})b_{-k}^*a_k^*|\psi_0\rangle$$

$$=\Omega_k b_{-k}^*a_k^*|\psi_0\rangle. \quad (7.5)$$

In the last step the commutation rule (2.4) was used, and the property $a_p|\psi_0\rangle=0$. The second-order correction to the wave function agrees in the two pictures, and is a sum of terms of the form $b_{-k}^*a_k^*|\psi_0\rangle$ with various coefficients. The third-order term for $|\psi\rangle$ is obtained by another application of BH_I. The effect of H_I is to give terms like $(b_{-l}^*a_l^*)(b_{-k}^*a_k^*)|\psi_0\rangle$, $b_k^*b_{-k}^*|\psi_0\rangle$, and $a_k^*a_{-k}^*|\psi_0\rangle$, and application of $K-H_0'$ and T gives the same result, by the argument used in (7.5). The argument breaks down only when the boson commutation rule is not true, which occurs when T acts on a state not in S. H_I acting once on $|\psi_0\rangle$ gives a state containing holes of minimum absolute momentum k_f-k_c. Each successive H_I lowers the minimum by k_c, so after k_f/k_c steps of H_I the holes are in the critical region near $k=0$, and this part of $|\psi\rangle$ is not in S. In the series (7.2) for the energy shift we can let B act either to the left or right. The Tomonaga model $|\psi\rangle$ is therefore correct to order k_f/k_c and the energy E to order $2k_f/k_c$. For the one-quantum excited state of the normal modes of Sec. 4 these limits are $(k_f-k_c)/k_c$ and $2(k_f-k_c)/k_c$, respectively.

The second-order diagrams for the energy shift ΔE are shown in Figs. 5 and 7 in the electron and density wave pictures. That these diagrams are equal can be seen from the results of Sec. 6, where the contribution of the electron-picture diagram was (6.6)

$$-\frac{1}{L}\sum_{|k|<k_c,p,\sigma}\frac{g_k^2}{2\omega_k}(\Omega_k+\omega_k)^{-1}.$$

From the particle and hole restrictions on (6.6), p must lie for $k<0$ between k_f and $k_f+|k|$ and for $k>0$ between $-k_f$ and $-(k_f+|k|)$. The sum over p gives the factor $(L/2\pi)|k|$, and the remaining sum over k, σ is the result (6.8) for the contribution of the density wave diagram which may be called a Tomonaga diagram. The density wave propagator (dashed line) therefore sums up the electron-hole bubbles of the first diagram for different p. The Tomonaga diagrams have the structure of particle-hole bubbles linked to phonons at both ends. The method of Sawada[13] can be used to sum these diagrams, but the procedure cannot be justified from the Sawada Hamiltonian in which each particle-hole pair of momenta $p+k$, p is treated as a boson. It is only the coherent superposition of pairs with different p that behaves as a boson density wave.

In the fourth order there are six diagrams in the electron picture shown in Fig. 8, from which all the fourth-order Tomonaga diagrams with the same contributions are obtained if the bubbles are replaced by dashed lines. There are twelve extra diagrams which fall into two groups of six, and each group is the "time-reversed" image of the other. One of the groups is shown in Fig. 9. Time reversal reverses the arrows in a diagram, so that electrons become holes, and vice versa. The contribution of a diagram is unchanged under time reversal, from the particle-hole symmetry about the Fermi level.

Since the Tomonaga energy should be correct to high order, the sum of the contributions of the extra diagrams is zero, even for an arbitrary phonon spectrum ω_k and coupling g_k. The phonon structure determines the matrix elements and the intermediate-state energy. The excitation energy of the particles and holes is proportional to the magnitude of the excitation momentum, which equals the magnitude of the net phonon momentum. This means we can fix the phonon momenta in the diagrams, and group the diagrams of the same phonon structure in time when all the particle and hole lines are removed. Since Fig. 9(a) is the only diagram

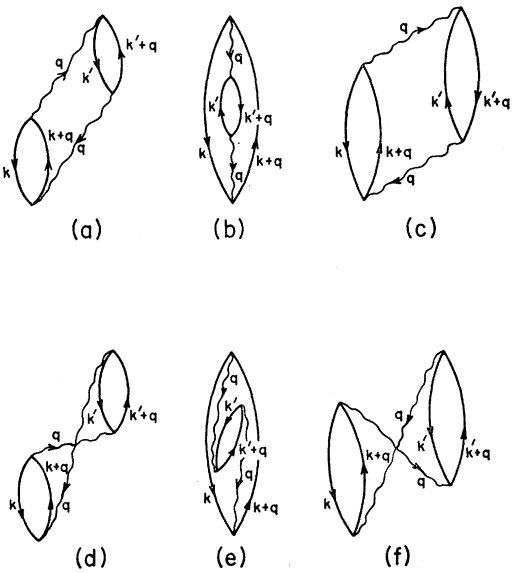

FIG. 8. The six Tomonaga diagrams which occur in fourth-order perturbation drawn in the electron picture.

[13] K. Sawada, Phys. Rev. 106, 372 (1957).

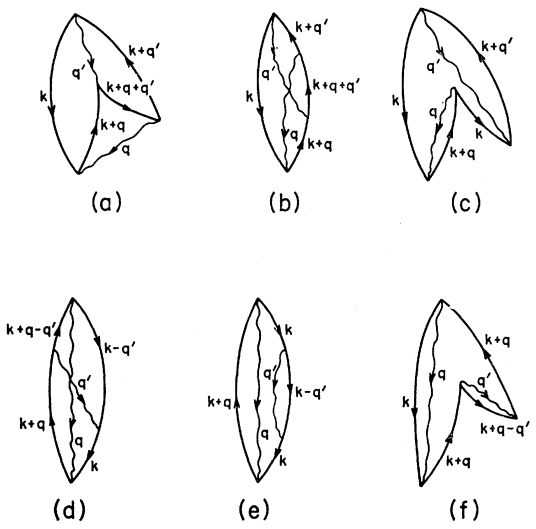

FIG. 9. The six non-Tomonaga diagrams which occur in fourth order.

with no phonons present in the second intermediate state, it forms a group with one member, and so must be zero. The requirement that holes be in the sea and particles outside places the following restrictions on its momenta if we choose k positive:

$$\text{(i) } k<k_f, \quad \text{(ii) } k+q+q'<k_f,$$
$$\text{(iii) } k+q>k_f, \quad \text{(iv) } k+q'>k_f.$$

Adding (i), (ii), and the negative of (iii), we obtain $k+q'<k_f$ contradicting (iv). The sum over momenta of diagram 9(a) is vacuous.

The diagrams of Figs. 9(b) and (c) form the second group. The sign rule gives minus and plus, respectively. It remains to check that the restrictions on momenta are identical. For (b),

$$\text{(i) } k+q>k_f, \quad \text{(ii) } k<k_f,$$
$$\text{(iii) } k+q'>k_f, \quad \text{(iv) } k+q+q'>k_f.$$

For (c),

$$\text{(i) } k+q>k_f, \quad \text{(ii) } k<k_f, \quad \text{(iii) } k+q'>k_f.$$

The condition (iv) of (b) can be obtained by adding (i) and (iii) and subtracting (ii).

In the last group of Figs. 9(d), (e), (f) the signs are $+, -, +$. The momentum conditions are:
For (d),

$$\text{(i) } k<k_f, \quad \text{(ii) } k-q'<k_f,$$
$$\text{(iii) } k+q>k_f, \quad \text{(iv) } k+q-q'>k_f.$$

For (e),

$$\text{(i) } k<k_f, \quad \text{(ii) } k-q'<k_f, \quad \text{(iii) } k+q>k_f.$$

For (f),

$$\text{(i) } k<k_f, \quad \text{(iii) } k+q>k_f, \quad \text{(v) } k+q-q'<k_f.$$

Now (v)+(i)−(iii) gives (ii). Given (i), (ii), and (iii), then one and only one of (iv) and (v) is true, so diagrams (d) and (f) cancel (e).

The same kind of cancellation must occur in higher orders, although it becomes quite difficult to check directly. We can characterize the diagrams which are not included in Tomonaga, and which do not cancel, but give corrections to the Tomonaga energy E_T. The diagrams in a specific phonon structure group in an order less than $r=2k_f/k_c$ add to zero, and contain no hole lines which scatter from one side of $k=0$ to the other. Now consider a group of high enough order so that this scattering is present, for example, one such that the hole moves from $k>0$ to $k<0$ and back. If we imagine increasing k_f sufficiently, the structure of these diagrams does not change, but the hole stays entirely on the side $k>0$; the group then has order less than the new r and so gives zero. Setting k_f equal to its original value, we see that the reason the group does not cancel is due to the kink in the energy-momentum relationship ϵ_k as k passes through zero. The energy of the intermediate state when the hole is near $k=0$ is at least the Fermi energy E_f. The effect of the kink in ϵ_k in a specific diagram is negligible until the change caused by it is comparable to E_f, so the hole has moved over near to $-k_f$; this argument is also valid for several such holes. If the order of perturbation theory is above $2r$ we obtain diagrams of a new structure. For example, a hole which started near k_f moves all the way over to $-k$ in many stages and is annihilated there by a particle. But these diagrams have many intermediate-state energies above E_f, and thus represent a very small correction to E_T.

8. THE ELECTRON DISTRIBUTION

The perturbation expansion of the electron distribution in the momentum space may be obtained from the formula

$$\begin{aligned}\langle\psi|n_{l,\sigma}|\psi\rangle&=\langle\psi|c_{l,\sigma}{}^*c_{l,\sigma}|\psi\rangle\\&=\lim_{S\to\infty}\langle e^{-HS}n_{l,\sigma}e^{-HS}\rangle/\langle e^{-2HS}\rangle\\&=\lim_{S\to\infty}\left\langle \mathcal{T}\exp\int_S^{2S}-H_I(u)du\,n_{l,\sigma}(S)\right.\\&\quad\left.\times\exp\int_0^S-H_I(t)dt\right\rangle\Big/\\&\qquad\left\langle\mathcal{T}\exp\int_0^{2S}-H_I(t)dt\right\rangle. \quad (8.1)\end{aligned}$$

In the expansion there must be an even number of H_I in each term, so the sign is determined by the parity of the contraction. The contraction $:c_{l,\sigma}{}^*(S)c_{l,\sigma}(S):$ gives exactly $\langle n_{l,\sigma}\rangle$ which is 1 or 0 as l is inside or outside the sea.

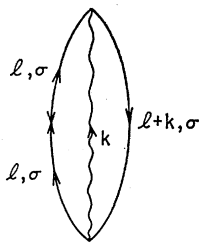

FIG. 10. Second-order diagram for the occupation number of a particle state.

The lowest order contraction of $c_{l,\sigma}{}^{*}c_{l,\sigma}$ with the H_I can be represented by the diagram of Fig. 10 in the case $|l|>k_f$. The x on the particle line of momentum l, spin σ denotes the effect of $n_{l,\sigma}(S)$ in first removing the particle in state l and then returning it. When the x appears on a hole line there is an extra -1 in the parity. The time integration leads to the square of the intermediate-state energy appearing in the denominator. The contribution of the diagram is

$$\frac{1}{L}\sum_k \frac{g_k{}^2}{2\omega_k}(\omega+\epsilon_l-\epsilon_{l-k})^{-2}$$

$$=\frac{\alpha^2}{32}\left[\frac{1}{1+\Omega_{l-k_f}/\omega}-\frac{1}{1+x}\right], \quad |l-k_f|<k_c$$

$$=0, \qquad |l-k_f|>k_c. \quad (8.2)$$

If $|l-k_f|>k_c$ there is no phonon momentum large enough to put the hole in the sea.

The linked-cluster theorem for this expansion is valid, and the diagrams differ from those for the ground-state energy only by the presence of an x in some intermediate state on a particle (hole) line if $|l|>k_f$ $(<k_f)$, which requires this line to have momentum l and spin σ. The excitation energy of the intermediate state with the x appears squared in the denominator.

In second order we have the Tomonaga diagram of Fig. 5. In fourth order the x can be put on the Tomonaga diagrams of Fig. 8 as well as on the extra diagrams of Fig. 9. Is it reasonable to expect that the Tomonaga diagrams provide as good a description of the electron distribution as of the ground-state energy? This cannot be true, because the Tomonaga diagrams give no contribution to $\langle\psi|n_l|\psi\rangle$ if $|l|>k_f+k_c$ or $|l|<k_f-k_c$, since the highest momentum particle in such a diagram is at k_f+k_c and the lowest momentum hole at k_f-k_c. It has been pointed out in Sec. 7 that the second-order term in the expansion of ψ already has holes down to momentum k_f-2k_c. There are two reasons why the extra diagrams of Fig. 9 with the x on some line no longer cancel. Diagrams like Fig. 9(c) have two particles or holes in one intermediate state, and the x can be placed on either. In addition, the x fixes the momentum of a line, which can restrict the phase space of two canceling diagrams (without the x) in different ways.

In the Tomonaga model the electron-phonon coupling has no effect on the paramagnetic susceptibility χ. The term added to the Hamiltonian is $\Delta H=\mu B(N_\uparrow-N_\downarrow)$, where $N_\uparrow$ $(N_\downarrow)$ is the number operator for spin-up (down) electrons, μ the electron magnetic moment, and B the magnetic field. This term commutes with the (zero-field) electron-phonon Hamiltonian. In the Tomonaga model we let ψ_0 be the ground state of $K+H_s+\Delta H$ and apply the perturbation expansion (7.1) in the density wave picture. The essential property of the ψ_0, namely $a_p|\psi_0\rangle=0$ is still true, and the expansion for ΔE of (7.2) is unchanged. Therefore the ground-state energy shift due to the magnetic field is all present in the uncoupled system. The change in susceptibility due to electron-phonon coupling in a system with electron spectrum $p^2/2m$ comes about from the curvature of the kinetic energy around the Fermi level. In the weak-coupling limit the fractional change in χ due to the phonons and the curvature is of the order of $\alpha^2(\omega/E_f)^2$.

9. GREEN'S FUNCTION APPROACH TO THE TOMONAGA MODEL

We have seen that the evaluation of the ground-state energy in the Tomonaga model corresponds to a summation of the bubble diagrams for the electron-phonon system. The Green's function approach to the electron-phonon problem[14] may be used to sum bubble diagrams. We use the Pauli-Feynman[15] technique to write the ground-state energy in terms of Green's functions

$$\langle H\rangle=\langle H_0\rangle_{g=0}+\int_0^g \frac{dg'}{g'}\Big\langle\sum_{k,q,\sigma}\frac{g'}{(2\omega)^{1/2}}c_{k+q,\sigma}{}^{*}c_{k,\sigma}\times(b_q+b_{-q}{}^{*})\Big\rangle$$

$$=\langle H_0\rangle_{g=0}+i\int_0^g\frac{dg'}{g'}\int\frac{d^2k}{(2\pi)^2}\Pi(k)D(k), \quad (9.1)$$

where

$$\langle H_0\rangle_{g=0}=2\sum_{k<k_f}\epsilon_k+\tfrac{1}{2}\sum_k\omega_k. \quad (9.2)$$

To sum only bubble diagrams, the vertex function is chosen to be 1. The phonon self-energy is

$$\tilde{\Pi}(k)=-2ig^2\int(2\pi)^{-2}d^2pG_0(p+k)G_0(p),$$

$$=-2ig^2\int(2\pi)^{-2}d^2p[p_0+k_0-\epsilon(p+k) \quad (9.3)$$

$$+i\delta\epsilon(p+k)]^{-1}[p_0-\epsilon(p)+i\delta\epsilon(p)]^{-1},$$

$$=4g^2N(0)\Omega^2(k)/[k_0{}^2-\Omega^2(k)+i\delta], \quad \delta=0^{+},$$

[14] A. A. Abrikosov, L. P. Gorkov, I. E. Dzyaloshinski, *Methods of Quantum Field Theory in Statistical Physics* (Prentice Hall, Inc., Englewood Cliffs, New Jersey, 1963), pp. 93.

[15] W. Pauli, *Handbuch der Physik*, edited by S. Flügge (Julius Springer, Berlin, 1933), 2. Aufl. XXIV/1, pp. 161; R. P. Feynman, Phys. Rev. **56**, 340 (1939).

where we have made the linear energy approximation

$$\epsilon(p-k)-\epsilon(p)=\pm\Omega(k)=\pm v_f|k|\,, \tag{9.4}$$

and as before $N(0)=1/2\pi v_f$.

The phonon Green's function $\tilde{D}$ is given by

$$\begin{aligned}\tilde{D}(k)&=(D_0^{-1}(k)-\tilde{\Pi}(k))^{-1}\\&=(k_0^2-\Omega^2)[(k_0^2-\omega^2)(k_0^2-\Omega^2)\\&\qquad-4g^2N(0)\Omega^2+i\delta]^{-1}.\end{aligned} \tag{9.5}$$

The poles of $\tilde{D}$ correspond to the perturbed excitations (4.9) and (4.10) found in the Tomonaga model

$$\tilde{D}(k)=(k_0^2-\Omega_k^2)[(k_0^2-\Lambda_k^2)(k_0^2-\lambda_k^2)+i\delta]^{-1}.$$

The addition to the ground-state energy arising from the interaction is

$$\begin{aligned}E_{\rm int}&=i\int_0^g\frac{dg'}{g'}\int\frac{d^2k}{(2\pi)^2}\tilde{\Pi}(k)\tilde{D}(k)\\&=i\sum_k\int_0^g\frac{dg'}{g'}\int_{-\infty}^{\infty}\frac{dk_0}{2\pi}\frac{4g'^2N(0)\Omega^2}{(k_0^2-\Lambda^2)(k_0^2-\lambda^2)+i\delta}\\&=\sum_k\int_0^{g^2}dg'^2N(0)\Omega^2\left[\frac{1}{\Lambda(\Lambda^2-\lambda^2)}+\frac{1}{\lambda(\lambda^2-\Lambda^2)}\right].\end{aligned} \tag{9.6}$$

Now consider the dependence of Λ and λ on g'^2, using (9.9), (9.10), and (9.11)

$$d(\Lambda+\lambda)=4N(0)\Omega^2\left[\frac{1}{\Lambda(\Lambda^2-\lambda^2)}+\frac{1}{\lambda(\lambda^2-\Lambda^2)}\right]\frac{dg'^2}{2}. \tag{9.7}$$

With this one may transform (9.6).

$$E_{\rm int}=\tfrac{1}{2}\sum_k\int_{\omega+\Omega}^{\Lambda+\lambda}d(\Lambda'+\lambda')=\tfrac{1}{2}\sum(\Lambda+\lambda-\omega-\Omega). \tag{9.8}$$

The expression for the ground-state energy is then identical with (9.14)

$$\langle H\rangle=2\sum_{|k|<k_f}\epsilon_k+\tfrac{1}{2}\sum(\Lambda+\lambda-\Omega). \tag{9.9}$$

It is not very surprising that one could use Green's functions to obtain this result. The fact which is surprising is that we have a model in which we can obtain many quantities simply to any desired order of perturbation theory. One such quantity is the phonon Green's function, D. D may be calculated once its spectral function is known. The spectral function in turn depends only upon the matrix element of the phonon creation operator taken between the ground state and any excited states of the system. By our previous analysis we know that the ground-state wave function is given correctly to a high order of perturbation theory when only bubble diagrams are included. Each phonon operator can be written in terms of two normal-mode operators using (4.5), (4.6), and (4.12). Each of the two excited states we can go to is correctly given to one order lower in the coupling constant than is the ground-state wave function, as shown in Sec. 7.

Since D is correct and

$$D(k)=[D_0^{-1}(k)-\Pi(k)]^{-1},$$

we then must have

$$\Pi(k)=\tilde{\Pi}(k)+O((g^2N(0)/\omega^2)^{k_f/k_c}). \tag{9.10}$$

Our expression for $\tilde{\Pi}$, 9.3, involves only g^2. Thus there must be an exact cancellation of all diagrams of order higher than second and up to order $2k_f/k_c$. Consequently we may write

$$\int dp_0\Pi(p)D(p)=\int dp_0\tilde{\Pi}(p)\tilde{D}(p)+O(g^{2k_f/k_c}). \tag{9.11}$$

An equivalent way of writing (9.11) is

$$\int dp_0\Sigma(p)G(p)=\int dp_0\tilde{\Sigma}(p)G_0(p)+O(g^{2k_f/k_c}), \tag{9.12}$$

since the left-hand sides of (9.11) and (9.12) are two ways of calculating the expectation of the interaction term

$$\left\langle\sum_{|q|<k_c,\sigma}\frac{g_q}{(2\omega_q)^{1/2}}c_{p+q,\sigma}{}^*c_{p,\sigma}(b_q+b_{-q}{}^*)\right\rangle.$$

The right-hand sides of (9.11) and (9.12) are identical by definition. The quantities $\tilde{\Sigma}$, $\tilde{\Pi}$, and $\tilde{D}$ are obtained from the Dyson equations for Σ, Π, and D by replacing the vertex function Γ by 1 and the electron Green's function G by the noninteracting one G_0. Although the expressions for D and Π in terms of bubble diagrams only are correct, the expression for Σ is not. $\tilde{\Sigma}$ is an incorrect expression for Σ starting at fourth order; only the combination $\int dp_0\tilde{\Sigma}(p)G_0(p)$ is correct to order $2k_f/k_c$. For fixed cutoff we see that the order of perturbation theory to which the various quantities are exact can be made arbitrarily high by increasing the density of the system.

10. POSSIBILITY OF EXTENSION TO THREE DIMENSIONS

In this section we attempt to carry the diagrammatic analysis we have used in the one-dimensional model on to three dimensions. A number of workers in the past have calculated the ground-state energy of a three-dimensional system with electron-electron interactions by summing only bubble diagrams.[16]

[16] M. Gell-Mann and K. A. Brueckner, Phys. Rev. **106**, 364 (1957); K. Sawada, Ref. 13; K. Sawada, K. A. Brueckner, N. Fukuda, and R. Brout, Phys. Rev. **108**, 507 (1957); R. Brout, *ibid.* **108**, 515 (1957); J. Hubbard, Proc. Roy. Soc. (London) **A240**, 539 (1957); **A243**, 336 (1958); P. Nozières and D. Pines, Phys. Rev. **109**, 1009 (1958).

We have seen in Sec. 7 that the existence of the Tomonaga operators required the sum of the contributions of sets of diagrams to vanish. The structure of the diagrams does not depend on the dimensionality of space. In second order there is only one diagram, which is of the bubble type. In fourth order there are 12 diagrams not of the bubble type.

We will state the results before going into the details of the integrations. There is *not exact* cancellation of the non-Tomonaga diagrams. This is independent of the ratio k_c/k_f.

The other results are model-dependent; we choose a constant optical-phonon spectrum energy ω, constant matrix element $g_k=g$, and a cutoff on momentum transfer, $k_c=x\omega/v_f$; x is a number having the same meaning as in Sec. 3, and is taken equal to 2. In metals the ratio of the maximum phonon energy to the Fermi energy is a small number, approximately 10^{-2}. The electron kinetic energy is chosen to be $\epsilon(k)=k^2/2m$. The ratio of the sum of Tomonaga diagrams to the sum of non-Tomonaga diagrams is of the order $(E_f/\omega)^3$. Thus, although there are no boson operators which diagonalize the Hamiltonian exactly in fourth order, there is the possibility of operators which may be used to calculate fourth order to one part in 10^6.

Let us first consider the contribution of the Tomonaga diagram in Fig. 8(e). Figure 8(f) has the same number of particles, holes, and phonons in each intermediate state and can be treated in the same way.

$$\Delta E_{8e}=-\frac{4g^4}{4\omega^2}\int\frac{d^3kd^3k'd^3q}{(2\pi)^9}\left(\frac{\mathbf{k}\cdot\mathbf{q}}{m}+\omega\right)^{-2}\times\left(\frac{(\mathbf{k}+\mathbf{k}')\cdot\mathbf{q}}{m}+2\omega\right)^{-1}. \quad (10.1)$$

The factor of 4 in the numerator comes from the sum over spins. We neglect terms $q^2/2m<k_c^2/2m=\omega k_c/k_f$ which occur in the energy denominators, since they are down by a factor k_c/k_f relative to ω. These terms arise from differences of electron kinetic energies $\epsilon(k+q)-\epsilon(k)$. We may now easily place upper and lower bounds on the integral, since for all allowed values of $\mathbf{k}\cdot\mathbf{q}$ and $\mathbf{k}'\cdot\mathbf{q}$,

$$\tfrac{1}{2}\omega^{-3}(1+x)^{-3}\leq\left(\frac{\mathbf{k}\cdot\mathbf{q}}{m}+\omega\right)^{-2}\times\left(\frac{(\mathbf{k}+\mathbf{k}')\cdot\mathbf{q}}{m}+2\omega\right)^{-1}\leq\tfrac{1}{2}\omega^{-3}. \quad (10.2)$$

If we were to consider the contributions of diagrams 8(a) or 8(d), in which one of the intermediate states has two phonons but no particle-hole pairs, we would obtain as a lower bound of the integrand $\frac{1}{2}\omega^{-3}(1+x)^{-2}$ rather than the result given in (10.2). The contribution of any Tomonaga diagram of fourth order with phonons in the second intermediate state satisfies the inequality

$$\frac{g^4}{2\omega^5(1+x)^3}\int\frac{d^3kd^3k'd^3q}{(2\pi)^9}<|\Delta E_8|<\frac{g^4}{2\omega^5}\int\frac{d^3kd^3k'd^3q}{(2\pi)^9}. \quad (10.3)$$

Now we approximate the integral

$$J_8=\int d^3kd^3k'd^3q \quad (10.4)$$

subject to the restrictions

$$\begin{gathered}k'^2+q^2+2k'qz'>k_f^2,\quad z'=\hat{k}'\cdot\hat{q}\\ k^2+q^2+2kqz>k_f^2,\quad z=\hat{k}\cdot q\\ k^2<k_f^2,\quad k'^2<k_f^2.\end{gathered} \quad (10.5)$$

To order k_c/k_f we may relax these conditions to

$$\begin{gathered}qz'>k_f-k',\quad qz>k_f-k,\\ k<k_f,\qquad k'<k_f.\end{gathered} \quad (10.6)$$

The integrals are performed directly and the result for J is

$$J_8=(4/5)\pi^3k_f^4k_c^5[1+O(k_c/k_f)]. \quad (10.7)$$

The bounds are (10.3) are

$$\frac{E\mathfrak{U}}{27}<|\Delta E_8|<\left(\frac{g^2N(0)}{\omega^2}\right)^2\frac{\omega^4}{10\pi^2v_f^3}=E\mathfrak{U}, \quad (10.8)$$

where $N(0)=mk_f/2\pi^2$ is the three-dimensional density of states at the Fermi surface.

Before considering the two Tomonaga diagrams with no phonons in the second intermediate state we consider one of the non-Tomonaga diagrams with phonons in all intermediate states, Fig. 9(b). Actually a part of this diagram is cancelled by the diagram in 9(c), as we will see later. Even without this further suppression we will find we have gone down by a factor $(\omega/E_f)^2$.

$$\Delta E_{9b}=-\frac{2\times2g^4}{4\omega^2}\int\frac{d^3kd^3qd^3q'}{(2\pi)^9}\left(\frac{\mathbf{k}\cdot\mathbf{q}}{m}+\omega\right)^{-1}\times\left(\frac{\mathbf{k}\cdot\mathbf{q}'}{m}+\omega\right)^{-1}\left(\frac{\mathbf{k}\cdot(\mathbf{q}+\mathbf{q}')}{m}+2\omega\right)^{-1}. \quad (10.9)$$

The factor 2×2 comes from the sum over spins and the time-reversed diagram. We may put bounds on (10.9) as we did on (10.1).

$$\frac{g^4}{2\omega^5(1+x)^3}\int\frac{d^3kd^3qd^3q'}{(2\pi)^9}<|\Delta E_{9b}|<\frac{g^4}{2\omega^5}\int\frac{d^3kd^3qd^3q'}{(2\pi)^9}. \quad (10.10)$$

We do not impose the restriction $(\mathbf{k}+\mathbf{q}+\mathbf{q}')^2>k_f^2$ which is of higher order in k_c/k_f once the restrictions $(\mathbf{k}+\mathbf{q})^2>k_f^2$ and $(\mathbf{k}+\mathbf{q}')^2>k_f^2$ are satisfied.

To order k_c/k_f the restrictions on the integral

$$J_{9b}=\int d^3kd^3qd^3q' \tag{10.11}$$

are

$$qz>k_f-k,\quad q'z'>k_f-k,\quad k<k_f. \tag{10.12}$$

Performing the integrals we obtain

$$J_{9b}<2(2\pi)^3k_f^2k_c^7/27. \tag{10.13}$$

Comparing this result with (10.8) we see that $E_{9b}\approx(\omega/E_f)^2E_{\mathfrak{U}}$. This result is peculiar to three dimensions; it does not happen in one dimension. We can see this from a simple counting argument on the phase space available.[2] We label integration variables by k's if they are momenta of electrons at about the Fermi surface. The integration region is about k_c for k and also for the momentum transfers labeled by q's. A Tomonaga integral has the form

$$\int d^3kd^3k'd^3q\approx k_f^4\int_0^{k_c}q^4dq$$

in three dimensions, while a non-Tomonaga integral has the form

$$\int d^3kd^3qd^3q'\approx k_f^2\int_0^{k_c}q^6dq.$$

We have the relative factor $(k_c/k_f)^2$ quite simply. In the one-dimensional case, a Tomonaga integral is of the form

$$\int dkdk'dq\approx\int_0^{k_c}q^2dq.$$

A non-Tomonaga integral is of the form

$$\int dkdqdq'\approx\int_0^{k_c}q^2dq.$$

In one dimension all diagrams with phonons in all the intermediate states are of the same order of magnitude.

The Tomonaga diagrams we have not yet considered are those with no phonons in one intermediate state, Figs. 8(b) and 8(c). We will show that the bounds on the contributions of these diagrams are approximately the same as those obtained in (10.8). For both diagrams

$$g^4\omega^{-4}(1+x)^{-2}(2\pi)^{-9}J_{8'}<|\Delta E_{8'}|<\tfrac{1}{2}g^4\omega^{-4}(2\pi)^{-9}J_{8'}, \tag{10.14}$$

where the integral

$$J_{8'}=\int d^3kd^3k'd^3q\left(\frac{\mathbf{q}\cdot(\mathbf{k}-\mathbf{k}')}{m}\right)^{-1} \tag{10.15}$$

has the restrictions

$$k<k_f,\qquad k'>k_f,$$
$$qz'<k_f-k',\quad qz>k_f-k, \tag{10.16}$$

neglecting terms of order k_c/k_f. In the integrand we make the approximation

$$[\mathbf{q}\cdot(\mathbf{k}-\mathbf{k}')/m]^{-1}\approx m[qk_f(z-z')]^{-1}.$$

The integrals over $\mathbf{k}$ and $\mathbf{k}'$ may be performed to give

$$J_{8'}=(2\pi)^2k_f^4m\int d^3qdzdz'qzz'[k_f(z-z')]^{-1}. \tag{10.17}$$

To within the order we are calculating to, the limits of integrations on the polar angles are obtained by setting k and $k'=k_f$ in (10.16).

$$0<z<1\quad -1<z'<0. \tag{10.18}$$

After changing the z' variable of integration to $-z'$ we have from (10.17) the following integral

$$\int_0^1dz\int_0^1dz'\frac{zz'}{z+z'}=\tfrac{2}{3}(1-\ln 2)\approx 0.2. \tag{10.19}$$

The q integration is trivial and we obtain

$$J_{8'}=0.1(2\pi)^3mk_f^3k_c^4. \tag{10.20}$$

The bounds on the contributions of these diagrams are evaluated using (10.14).

$$\tfrac{1}{9}E_{\mathfrak{U}}<|\Delta E_{8'}|<E_{\mathfrak{U}}. \tag{10.21}$$

Comparing this with (10.8) we find that all Tomonaga diagrams are of the same order of magnitude.

We next consider the sum of two non-Tomonaga diagrams which canceled in the one-dimensional case, Figs. 9(b) and 9(c). The energy denominators of the contributions from these two diagrams are not the same. For Fig. 9(b) we have

$$\Delta E_{9b}=-\frac{g^4}{\omega^2}\int\frac{d^3kd^3qd^3q'}{(2\pi)^9}\left(\frac{\mathbf{k}\cdot\mathbf{q}}{m}+\frac{q^2}{2m}+\omega\right)^{-1}\times\left(\frac{\mathbf{k}\cdot\mathbf{q}'}{m}+\frac{q'^2}{2m}+\omega\right)^{-1}\left(\frac{\mathbf{k}\cdot(\mathbf{q}+\mathbf{q}')}{m}+\frac{(\mathbf{q}+\mathbf{q}')^2}{2m}+2\omega\right)^{-1}, \tag{10.22}$$

whereas for 9(c) we have

$$\Delta E_{9c}=+\frac{g^4}{\omega^2}\int\frac{d^3kd^3qd^3q'}{(2\pi)^9}\left(\frac{\mathbf{k}\cdot\mathbf{q}}{m}+\frac{q^2}{2m}+\omega\right)^{-1}\times\left(\frac{\mathbf{k}\cdot\mathbf{q}'}{m}+\frac{q'^2}{2m}+\omega\right)^{-1}\left(\frac{\mathbf{k}\cdot(\mathbf{q}+\mathbf{q}')}{m}+\frac{q'^2}{2m}+\frac{q^2}{2m}+2\omega\right)^{-1}. \tag{10.23}$$

If we neglected the terms of order k_c/k_f smaller than ω in the denominators as we did previously, the denominators would be identical and then the sum of the two diagrams would give a contribution less than $E_{\mathfrak{U}}(\omega/E_f)^6$ in magnitude. However, (10.22) contains the term $\mathbf{q}\cdot\mathbf{q}'/m$ in the third factor not included in (10.23). We will expand (10.22) in terms of this factor, keeping only the first-order term

$$\Delta E_{9b+c}=-\frac{g^4}{\omega^2}\int\frac{d^3kd^3qd^3q'}{(2\pi)^9}\left(\frac{\mathbf{k}\cdot\mathbf{q}}{m}+\frac{q^2}{2m}+\omega\right)^{-1}\times\left(\frac{\mathbf{k}\cdot\mathbf{q}'}{m}+\frac{q'^2}{2m}+\omega\right)^{-1}\left(\frac{\mathbf{k}\cdot(\mathbf{q}+\mathbf{q}')}{m}+\frac{q^2+q'^2}{2m}+2\omega\right)^{-1}\times\left(-\frac{\mathbf{q}\cdot\mathbf{q}'}{m}\right)\left(\frac{\mathbf{k}\cdot(\mathbf{q}+\mathbf{q}')}{m}+\frac{q^2+q'^2}{2m}+\omega\right)^{-1}. \quad (10.24)$$

We may now drop all irrelevant terms

$$\Delta E_{9b+c}=\frac{g^4}{\omega^2}\int\frac{d^3kd^3qd^3q'}{(2\pi)^9}\left(\frac{\mathbf{k}\cdot\mathbf{q}}{m}+\omega\right)^{-1}\left(\frac{\mathbf{k}\cdot\mathbf{q}'}{m}+\omega\right)^{-1}\times\left(\frac{\mathbf{k}\cdot(\mathbf{q}+\mathbf{q}')}{m}+2\omega\right)^{-2}\frac{\mathbf{q}\cdot\mathbf{q}'}{m}. \quad (10.25)$$

The conditions on this integral are given in (10.12). An upper bound on (10.25) is

$$\Delta E_{9b+c}<g^4J_{9b+c}/4\omega^6(2\pi)^9m, \quad (10.26)$$

where

$$J_{9b+c}=\int d^3kd^3qd^3q'\mathbf{q}\cdot\mathbf{q}'. \quad (10.27)$$

We may use spherical trigonometry to obtain the cosine of the angle between $\mathbf{q}$ and $\mathbf{q}'$ in terms of z, z', and the angle φ between the projection of $\mathbf{q}$ and $\mathbf{q}'$ on a plane perpendicular to $\mathbf{k}$.

$$\mathbf{q}\cdot\mathbf{q}'=qq'(zz'+(1-z^2)^{1/2}(1-z'^2)^{1/2}\cos\varphi). \quad (10.28)$$

For an upper bound we weaken the conditions in (10.12) to $z>0$, $z'>0$,

$$J_{9b+c}<32\pi^3k_f^2k_c^9/45. \quad (10.29)$$

The result for the upper bound is

$$\Delta E_{9b+c}<\frac{8}{9}\left(\frac{\omega}{E_f}\right)^3E_{\mathfrak{U}}. \quad (10.30)$$

A result of the same order of magnitude is obtained from the sum of diagrams 9(d), (e), and (f). The contribution of Fig. 9(a) can be neglected since it can be shown to have a contribution no greater than $\approx(\omega/E_f)^5E_{\mathfrak{U}}$.

This completes the demonstration of the various assertions made at the beginning of this section. For this particular model there is little doubt that the Tomonaga diagrams give the most important contribution to the ground-state energy. Since the phase space suppresses long wavelengths the statement above can only be true for a physical system if the matrix element g_k emphasizes long-wavelength interactions.

11. CONCLUSIONS

The Tomonaga method provides a technique for obtaining a number of quantities to an arbitrarily high order of perturbation theory in certain one-dimensional electron-phonon models. In three dimensions the bubble diagrams which occurred in the Tomonaga method do not sum terms beyond second-order perturbation theory exactly, but to a very high approximation in models which favor long-wavelength interactions.

ACKNOWLEDGMENTS

We should like to thank Professor Bardeen for originally suggesting an investigation of the Tomonaga model for comparison with the B.C.S. model of superconductivity in one dimension, and for discussions of the work. We would also like to thank Professor C. Bloch, Professor J. R. Schrieffer, and Professor G. Whitfield for their interest and helpful suggestions. This work made use of computer facilities supported in part by National Science Foundation Grant NSF-GP 579.